Journal of proteome research

Article

pubs.acs.org/jpr

Development of Isotope Labeling Liquid Chromatography Mass Spectrometry for Mouse Urine Metabolomics: Quantitative Metabolomic Study of Transgenic Mice Related to Alzheimer's Disease

Jun Peng,[†] Kevin Guo,[†] Jianguo Xia,[‡] Jianjun Zhou,[‡] Jing Yang,[∥] David Westaway,[∥] David S. Wishart,[‡,§,⊥] and Liang Li*[,†]

[†]Department of Chemistry, [‡]Department of Computing Science, [§]Department of Biological Sciences, and [∥]Centre for Prions and Protein Folding Diseases, University of Alberta, Edmonton, Alberta T6G 2R3, Canada

[⊥]National Institute of Nanotechnology, Edmonton, Alberta T6G 2M9, Canada

Supporting Information

ABSTRACT: Because of a limited volume of urine that can be collected from a mouse, it is very difficult to apply the common strategy of using multiple analytical techniques to analyze the metabolites to increase the metabolome coverage for mouse urine metabolomics. We report an enabling method based on differential isotope labeling liquid chromatography mass spectrometry (LC−MS) for relative quantification of over 950 putative metabolites using 20 μL of urine as the starting material. The workflow involves aliquoting 10 μL of an individual urine sample for ^{12}C-dansylation labeling that target amines and phenols. Another 10 μL of aliquot was taken from each sample to generate a pooled sample that was subjected to ^{13}C-dansylation labeling. The ^{12}C-labeled individual sample was mixed with an equal volume of the ^{13}C-labeled pooled sample. The mixture was then analyzed by LC−MS to generate information on metabolite concentration differences among different individual samples. The interday repeatability for the LC−MS runs was assessed, and the median relative standard deviation over 4 days was 5.0%. This workflow was then applied to a metabolomic biomarker discovery study using urine samples obtained from the TgCRND8 mouse model of early onset familial Alzheimer's disease (FAD) throughout the course of their pathological deposition of beta amyloid (Aβ). It was showed that there was a distinct metabolomic separation between the AD prone mice and the wild type (control) group. As early as 15−17 weeks of age (presymptomatic), metabolomic differences were observed between the two groups, and after the age of 25 weeks the metabolomic alterations became more pronounced. The metabolomic changes at different ages corroborated well with the phenotype changes in this transgenic mice model. Several useful candidate biomarkers including methionine, desaminotyrosine, taurine, N1-acetylspermidine, and 5-hydroxyindoleacetic acid were identified. Some of them were found in previous metabolomics studies in human cerebrospinal fluid or blood samples. This work illustrates the utility of this isotope labeling LC−MS method for biomarker discovery using mouse urine metabolomics.

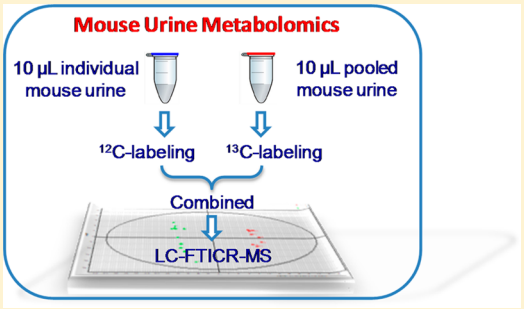

KEYWORDS: *Alzheimer's disease, mouse model, mouse urine, isotope labeling, LC−MS, metabolomics*

INTRODUCTION

Alzheimer's disease (AD) is one of the most common neurodegenerative disorders in the elderly.[1] Currently, there is no effective treatment for AD. Furthermore, there are no definitive biomarkers for the reliable clinical diagnosis of AD at the early stage of development, although late-stage AD can be diagnosed using MRI brain scans and protein biomarkers in cerebrospinal fluid.[2−4] The difficulty in diagnosing AD may arise from the complex perturbations occurring in the genome, transcriptome, proteome, and metabolome of the affected individuals. While most AD biomarker studies have focused on transcriptomic or proteomic assays, metabolomic assays may prove to be sensitive enough to distinguish AD phenotypes from normal.[5−7] Traditional biochemical studies have shown that neurodegenerative disorders are often linked to disturbances in metabolic pathways related to neurotransmitter synthesis,[8,9] oxidative stress,[10] and mitochondrial function.[11] Metabolome analysis with a broad metabolite coverage may allow us to monitor metabolite perturbations in many biochemical pathways and to discover a panel of metabolite biomarkers specific to AD.

Over the past few years, a significant number of metabolomics studies on AD have been reported. These include animal models as well as human studies. In human studies, most investigated cerebrospinal fluid (CSF) sam-

Received: August 6, 2014
Published: August 28, 2014

   dx.doi.org/10.1021/pr500828v | J. Proteome Res. 2014, 13, 4457−4469

ples,[12−15] plasma samples,[15−18] or brain samples.[19] In animal models, brain tissues of mouse models were most commonly used.[20−22] Two mouse model studies used both brain and plasma.[23,24] All these studies indicated the metabolomic changes associated with AD and showed the initial promise of metabolomics techniques in the investigation of AD disease. The analytical techniques employed include LC−electrochemical array (ECA),[12,13] GC−MS,[23] LC−MS,[16,18,19,22] capillary electrophoresis (CE)−MS,[25] and NMR.[20,24] However, each of these techniques could only detect a relatively small number of metabolites. There is a need to develop more sensitive and quantitative metabolomic approaches to search for biomarkers of AD. We have recently reported a quantitative metabolomic technique based on ^{13}C-/^{12}C-isotope dansylation labeling combined with LC Fourier-transform ion cyclotron resonance (FTICR) MS.[26,27] Dansylation is a chemical derivatization method that greatly enhances the electrospray ionization (ESI) signal response and improves reversed-phase (RP) LC separation and, hence, offers much more comprehensive metabolome coverage. Furthermore, the introduction of ^{13}C-/^{12}C-isotope tags enables relative (and absolute) quantification by isotope dilution with much improved measurement precision. This method has been successfully applied for analyzing biological samples, including human CSF,[27] human urine,[28] human saliva,[29] and bacterial cells.[30,31]

Urine metabolomics in a transgenic mice model of AD has not been extensively studied. Only one urine metabolomics study of mouse model of AD using NMR was reported very recently.[32] Because of a limited volume of urine available from a mouse, it is technically challenging to perform urine metabolomics with high metabolome coverage. However, due to the noninvasive nature of sample collection, urine is an excellent source for metabolomics, especially if one wishes to find a set of noninvasive early stage diagnostic biomarkers, which could be complementary to biomarkers in CSF, blood, or brain tissue. Here we report a quantitative metabolomics approach based on differential ^{13}C-/^{12}C-isotope labeling combined with LC−FTICR−MS for urinary biomarker discovery in a transgenic mouse model of AD.

EXPERIMENTAL SECTION

Chemicals and Reagents

All the chemicals and reagents, unless otherwise stated, were purchased from Sigma-Aldrich Canada (Markham, ON, Canada). For dansylation labeling reactions, the ^{12}C-labeling reagents were from Sigma-Aldrich and the ^{13}C-labeling reagents were synthesized in our lab using the procedures published previously.[26] LC−MS grade water, methanol, and acetonitrile (ACN) were purchased from ThermoFisher Scientific (Nepean, ON, Canada).

Mouse Model and Sample Collection

The TgCRND8 transgenic mice (see Results and Discussion for more information) were used in this study. The strains of all the mice were 129Svev, and the mice were fed with 4% mice chow. The urine samples were collected at three different ages, namely 15−17 weeks, 25−28 weeks, and 30−31 weeks. Table 1 shows the sample information about the mouse urine samples. To avoid possible contamination with bedding material and animal waste, the urine samples were collected by lifting the mouse one-by-one from the home cage and immediately placing into a brand new disposable plastic cage (Innovive Inc. San Diego, CA). The mouse was left inside the empty cage to urinate spontaneously, usually within 5 min but occasionally with an interval of up to 30 min. Immediately after the mouse had urinated, urine was pipetted from the floor of the cage into a 1.5 mL Eppendorf tube and snap-frozen on dry ice.

Table 1. Information on the Mouse Urine Samples Used in This Study

total no. of mice	24		
no. of mice (male and female)		12 male	12 female
no. of mice (APP mutant and wild type)		12 APP	12 WT
total no. of samples (APP mutant and WT)	75	39 APP	36 WT
at the ages of 15−17 weeks	28	15 APP	13 WT
at the ages of 25−28 weeks	23	12 APP	11 WT
at the ages of 30−31 weeks	24	12 APP	12 WT

It should be noted that using metabolic cages for collection of 24 h urine is commonly done in metabolomics. In our current work, mouse urine was collected at a fixed time interval during the day, between 1:00 and 3:00 pm, and 6−8 h into the daytime light cycle of the caged animals. While it is likely that metabolites produced in mice fed *ad libitum* will still vary on a diurnal rhythm, this sampling method with a 2 h time window makes any error a systematic one. On 24 h urine collection, urine metabolites over a 24 h period are pooled and thus diurnal changes cannot be discerned either. One potential drawback of 24 h collection is that labile metabolites may degrade or oxidize during the sample collection period, whereas samples produced by the protocol here are snap-frozen. Recent work suggested that freezing urine samples is important to reduce metabolome changes during the sample collection process.[33] We note that because our technique is sufficiently sensitive to handle a small volume of urine from an animal without the need of pooling, in the future we will compare 2 h time window urine collection at various hours with the 24 h urine collection method to examine any metabolome variations caused by diurnal variation and collection methods.

Sample Preparation

Figure 1 shows the experimental workflow for sample preparation and LC−MS analysis. A pooled sample was created by aliquoting 10 μL of each of the 75 mouse urine samples and mixing them well. The method for dansylation labeling of urine was adapted from our previous report.[26] Briefly, 10 μL of individual mouse urine sample or 10 μL of the pooled sample was diluted to 50 μL by adding 40 μL of water (LC−MS grade), then mixed with 50 μL sodium carbonate/sodium bicarbonate buffer (0.5 mol/L, pH 9.5) in reaction vials. A volume of 50 μL of freshly prepared ^{12}C-dansyl chloride solution (20 mg/mL) was added to each of the individual samples for light labeling. And 50 μL of ^{13}C-dansyl chloride solution (20 mg/mL) was added to each of the pooled sample for heavy labeling. The dansylation reaction was performed in an Innova-4000 benchtop incubator shaker at 60 °C for 60 min. To quench the reaction, 10 μL of the 250 mM sodium hydroxide solution was added. After additional 10 min incubation, the ^{12}C-dansylated individual sample was combined with the ^{13}C-dansylated pooled sample. The pH of the combined mixture was adjusted to pH 3 by adding formic acid. The mixture was then centrifuged for 10 min at 13 800*g* and was ready for LC−MS injection. A mixture of ^{12}C-dansylatated pooled sample and ^{13}C-dansylated pooled sample in 1:1 (v:v) was used as a quality control (QC) sample.

dx.doi.org/10.1021/pr500828v | J. Proteome Res. 2014, 13, 4457−4469

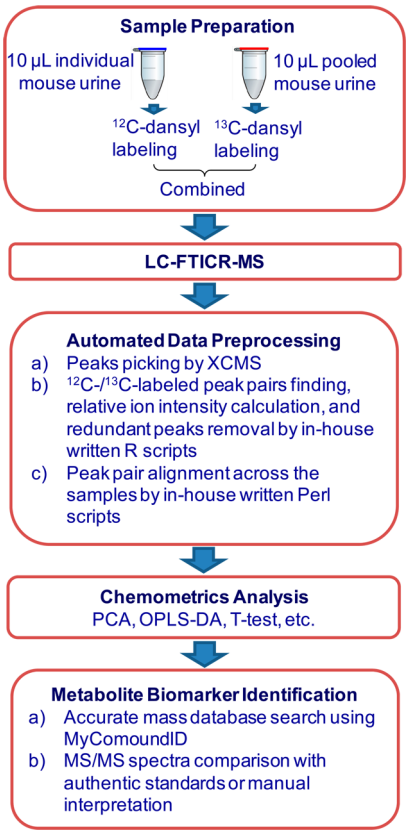

Figure 1. Experimental workflow of isotope labeling LC–MS for comparative metabolomics of mouse urine.

LC–MS

The HPLC system was an Agilent capillary 1100 binary system (Agilent, Palo Alto, CA). A reversed-phase Acquity BEH C18 column (1.0 × 100 mm, 1.7 μm particle size) was purchased from Waters (Milford, MA). LC Solvent A was 0.1% (v/v) formic acid in 5% (v/v) acetonitrile, and Solvent B was 0.1% (v/v) formic acid in acetonitrile. The gradient elution profile was as follows: t = 0 min, 20% B; t = 3.5 min, 35% B; t = 18 min, 65% B; t = 21 min, 95% B; t = 21.5 min, 95% B; t = 23 min, 98% B; t = 24 min, 98% B; t = 25.5 min, 20% B; t = 36.6 min, 20% B. The flow rate was 35 μL/min. The sample injection volume was 1.0 μL. To minimize the carryover and reduce the background noise peaks, a fast gradient elution of 22 min was run after each sample injection. The LC column was directly connected to a Bruker 9.4 T Apex-Qe FTICR mass spectrometer (Bruker, Billerica, MA) without splitting. The electrospray ionization (ESI) mass spectra were collected in the positive ion mode. The MS conditions used for FTICR-MS were as follows: nitrogen nebulizer gas, 2.3 L/min; dry gas flow, 7.0 L/min; dry temperature, 195 °C; capillary voltage, 4200 V; spray shield, 3700 V; acquisition size, 256 k; mass scan range, m/z 200–1000; ion accumulation time, 1 s; TOF (AQS), 0.007 s; DC extract bias, 0.7 V. All the urine samples were put into random order for injections. Eight injections of the QC sample (one QC injection after 9 sample injections) were used to monitor the performance of LC–MS running during the whole experiment.

We note that because of the slow data acquisition speed with the FTICR–MS instrument (1 spectrum/s) used to achieve optimal mass resolution and MS detection sensitivity, we compromised the chromatographic performance, that is, using a slower flow rate than optimal for LC separation. However, using the 1.7 μm particle size column, the chromatographic resolution is still good, which is demonstrated in the extracted ion chromatograms of two metabolites (m/z 592.1478 with base peak width of 15 s, and m/z 355.1476 with 20 s) in a labeled urine sample (see Supporting Information Figure S1).

For metabolite identification, an AB Sciex QTRAP 2000 hybrid triple-quadrupole with a linear ion trap mass spectrometer (Toronto, ON, Canada) was used to collect the MS/MS spectra of the interesting metabolites. The same LC system and column as those used in FTICR–MS were connected to this QTRAP MS.

Data Analysis

The LC–MS raw data were first converted to netcdf format using Bruker software DataAnalysis 4.0. The publicly available software XCMS[34] was used for peak picking. The XCMS parameters were set as fwhm = 3 and step = 0.005, sn = 1. An in-house written R program was used to find the ^{12}C-/^{13}C-isotopic pairs based on the mass difference of 2.00671 Da of isotopic pairs and the mass accuracy tolerance of 2 ppm. The relative ion intensity of ^{12}C-labeled/^{13}C-labeled pairs was calculated. The redundant peaks such as natural isotopic peaks, sodium adduct peaks, potassium adduct peaks, ammonia adduct peaks, dimer peaks, doubly charged peaks, and triply charged peaks were automatically removed by the program. We applied a threshold filter to remove noise peaks according to the background mass peak intensities. An in-house written Perl program was used to align or group the LC–MS data across the different urine samples, which was based on the mass accuracy tolerance of 5 ppm and retention time shift tolerance of 15 s. The table resulting from the Perl program contained the rows which were the individual samples and the columns which were the unique metabolites and their relative ion intensity between the individual sample and the pooled sample (i.e., peak ratios of ^{12}C-labeled/^{13}C-labeled pairs). The peak ratios of an individual sample were normalized to the total relative ion intensity to account for the urine volume dilution difference.

Multivariate statistical analysis of the LC–MS data was carried out using SIMCA-P+ 11.5 (Umetrics AB, Umea, Sweden). Principal components analysis (PCA), partial least-squares discriminant analysis (PLS-DA), and orthogonal projections to latent structures discriminant analysis (OPLS-DA) were used to analyze the data. Twenty permutation test and CV-ANOVA, built in SIMCA-P, were used to conduct cross validation for the PLS-DA and OPLS-DA models. A list of interesting metabolites that contributed mostly to the model was generated from the VIP list. The MetaboAnalyst[35] software was used to do the t test for the individual metabolite.

Metabolite Identification

Accurate mass of an underivatized metabolite was obtained by subtracting the measured mass of the dansylation labeled metabolite to the mass of the dansyl group. Based on the accurate mass information, the Human Metabolome Database (HMDB)[36] and the Evidence-based Metabolome Library (EML)[37] were searched using MyCompoundID,[37] with a mass accuracy tolerance of 5 ppm, to generate a list of mass-matched putative metabolites from the ion pairs detected. For positive metabolite identification, MS/MS spectra of the significant metabolites found to be differentially expressed in two groups were generated and manually interpreted. A metabolite was deemed to be definitively identified if the MS/MS spectrum and retention time matched with those of an

dx.doi.org/10.1021/pr500828v | J. Proteome Res. 2014, 13, 4457–4469

authentic standard. A metabolite was considered to be putatively identified if there was no authentic standard available.

RESULTS AND DISCUSSION

Mouse Model

Metabolomics has been applied to biomarker discovery in both human studies and animal studies. However, some confounding factors such as diet, environment and genetics can cause significant individual variability in human studies which complicate the biomarker discovery process.[38] On the other hand, animal models enable a much more controlled study and minimize the effects of confounding factors.[39] For studies of AD, an animal model would be expected to be particularly useful for identifying or generating a set of candidate markers that could be extended to human studies. Many transgenic mouse models of AD have been constructed based on the amyloid cascade hypothesis.[40,41] Amyloid beta (Aβ) plaque is one of the major pathophysiological features of AD. Aβ is the peptide fragment cleaved from an amyloid precursor protein (APP) by secretases. It aggregates extracellularly to form Aβ plaques, leading to neurodegeneration through a number of ill-defined neurotoxic mechanisms. Several transgenic mouse models expressing human mutant APP have been shown to develop amyloid plaque pathology and dense core plaques.[42] The TgCRND8 transgenic mouse model used in this study expresses a double mutant form of human APP 695 isoform and develops amyloid deposits as early as 2−3 months.[43] Therefore, the TgCRND8 transgenic mouse model allows one to perform AD biomarker discovery in a relatively short time period.

As Table 1 shows, we collected the urine samples at the ages of 15−17, 25−28, and 30−31 weeks to represent different stages of disease development. In this study, we did not collect the samples during the early development amyloid deposits during 8−12 weeks. Our cumulative studies with this Tg mouse line mimicking early onset familial AD (FAD) are that plaques can be seen from 65 days onward but multiple plaque deposits are present reliably but sparsely at 12 weeks of age, in accord with the description in Chishti et al.,[43] for example, more than one plaque deposit per sagittal section near the midline. This finding has not altered in moving our colony from one university to another and using (necessarily) slightly different conditions of husbandry. In this initial study to profile metabolites, we chose to start at a slightly "conservative" time point with respect to this model, that is, ∼4−6 weeks after the first documented chemical changes (plaque deposits, jump in Abeta levels detected by immunoblot or ELISA). Nonetheless, while future studies might assess our mice at yet earlier time-points, we note that gray matter Aβ deposition caused by FAD mutations is not associated per se with fulminant clinical disease; instead it reflects a preclinical event occurring about 15 years before symptom onset and about 10 years before onset of global cognitive impairment detected by mini-mental-state examination.[44] In short, our first time point can already be considered to equate to a preclinical state in the context of FAD.

Metabolome Profiling Method

The workflow of our quantitative metabolomics method for urine metabolomic biomarker discovery in a transgenic mice model is shown in Figure 1. This method is based on differential ^{13}C-/^{12}C dansylation labeling that was previously developed in our group. The method was able to detect and quantify over 600 metabolites in human urine in a single LC−MS run.[26] However, unlike human urine samples, the volume of mouse urine that can be conveniently collected without significant contamination from the environment is often limited. Collection of 20−50 μL per animal at a given time point is possible by removing mice from their home cage and placing them into a new disposable cage. This method does not cause any contact of urine on any surface inside the animal cage and thus prevents feces, food, and other species from contaminating the sample. The freshly collected urine sample can also be frozen immediately for storage, reducing the risk of bacterial growth and degradation of metabolites.

To handle the small volume of mouse urine (e.g., 10 μL), it was necessary to optimize the LC−FTICR−MS settings in order to achieve better detection of metabolites, as well as the dansylation labeling protocol. In this work, a 1 mm LC column, instead of a 2.1 mm column, was used, which could theoretically lower the detection limit by 4-fold. In addition, the ion accumulation time for data collection was optimized to be 1 s, instead of shorter time (e.g., <0.5 s). The limit of detection for the optimized LC−FTICR−MS method was found to be 0.24 nM for the dansylated phenylalanine. In the reported protocol,[26] dansylation labeling reaction requires a relatively large volume of sample, that is, 50 μL. It was found that merely scaling down the reaction volume from 50 to 10 μL could cause great variations in the mass spectrometric results, likely due to inhomogeneity of the reaction solution when 10 μL of urine was used. Instead, we diluted the mouse urine from 10 to 50 μL and kept all the reagent solution volumes the same as those used in the reported protocol. The detection of metabolome coverage was not compromised even when we started from 10 μL mice urine sample, since we have improved the limit of detection of the LC−MS method.

In our workflow, 20 μL of mouse urine was initially divided into two halves, with one half labeled by ^{12}C-dansylation and the other half combined with others to form a pooled sample that was labeled by ^{13}C-dansylation. Generally speaking, we could detect more than 950 unique ion pairs or putative metabolites in the mixture of the differentially labeled mice urine sample. Many of them could match with the metabolites in HMDB and EML, based on accurate mass search using 5 ppm mass error tolerance. For example, for the eight QC injections from the pooled sample, Supporting Information Table T1 shows the summary of the match results. Supporting Information Tables T2 and T3 list all the matches of the peak pairs to the HMDB and EML metabolite libraries, respectively. For the eight injections, the average number of peak pairs found was 1082 ± 148 (the peak pair number was lower for the first injection, likely due to insufficient conditioning of the column). There were a total of 1454 peak pairs detected from the combined results. About 92% of them could match with the metabolites in the two libraries. It is clear that our method can provide much better submetabolome coverage than a conventional LC−MS method. For example, 1942 features were detected in mouse urine in one study using UPLC−MS for metabolome profiling,[45] while another study reported the detection of 1412 features.[46] Since only a fraction of the features (less than 20%)[45] were actually from the true metabolites, these studies detected less than 400 metabolites. Among them, we would expect that only a fraction of them were from amines and phenols. In contrast, in our work, we routinely detected over 950 putative amine- and phenol-containing metabolites. However, the dansyl labeling LC−MS

dx.doi.org/10.1021/pr500828v | J. Proteome Res. 2014, 13, 4457−4469

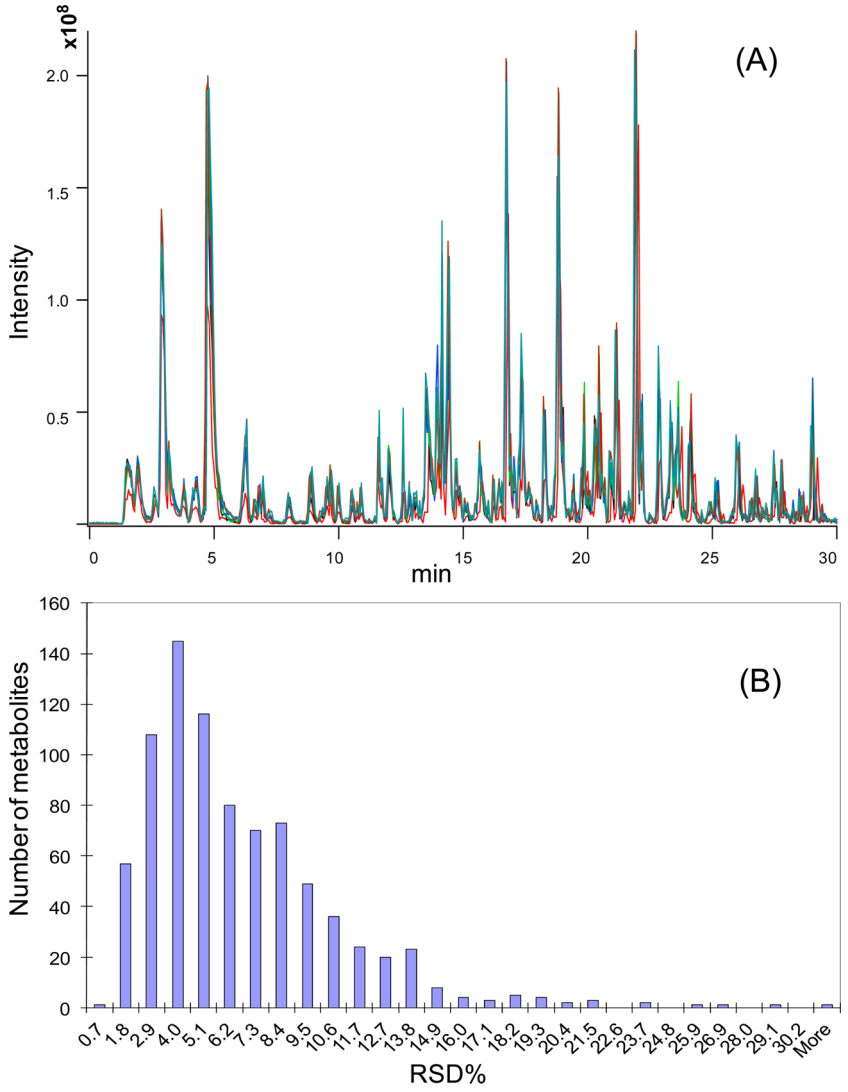

Figure 2. (A) Interday repeatability of overlaid base peak chromatograms of eight injections of quality control (QC) samples during 4 days LC−MS running; (B) frequency histogram of RSD% relative intensity of 840 metabolites in the QC samples.

method described in this work only detects the amine/phenol submetabolome. For detecting other groups of submetabolome, different labeling methods need to be used.[47]

Besides metabolite detectability, analytical variation of a global metabolomic profiling method should be minimized for biomarker discovery work, as a large analytical variation can mask the true biological variation between the disease state and the control state. We have evaluated the interday repeatability of our method using the pooled QC sample. Figure 2A shows the overlaid base-peak chromatograms of eight injections of the QC sample within 4 days. For these chromatograms, the maximum retention time shift within 4 days was less than 15 s. We randomly chose three metabolites from eight quality control samples to represent the relatively high, medium and low abundant metabolites, respectively. Supporting Information Table T4 shows that the retention time shift for these three different metabolites was 4.5, 1.1, and 12 s. The relative standard derivation (RSD) of the retention time was 0.15%, 0.04%, and 0.3%, respectively. We also evaluated the variation of the mass measurement within 4 days. The mass shift was 2.5, 1.4, and 1.1 ppm for these three different metabolites. These results indicate the FTICR−MS mass measurement with external calibration was quite stable within 4 days.

We calculated the RSD of the peak ratios individually for the 840 metabolites that were commonly detected in the eight injections, and the mean RSD was found to be 6.1% and the median RSD was 5.0%. Figure 2B shows the histogram of the frequency distribution of RSD% for the 840 metabolites. More than 96% metabolites have RSD% less than 15%, which was much better than the previously reported data using a label-free LC−MS method.[48,49] The better interday repeatability of our method is mainly due to the fact that we used ^{13}C-labeled pooled sample as a global internal standard, which could minimize the variations for the injection volume, electrospray response, instrumental settings, etc. We also investigated the experimental repeatability by running 3 replicates of dansylation reaction of a mouse urine sample (see Supporting Information Figure S2 for the overlaid base-peak ion chromatograms). The RSD% of peak ratios for all commonly detected metabolites was calculated. The mean RSD was 10.7%, and the median RSD was 7.4%. These results indicate that, despite the use of a small volume of urine sample (10 μL for labeling),

dx.doi.org/10.1021/pr500828v | J. Proteome Res. 2014, 13, 4457−4469

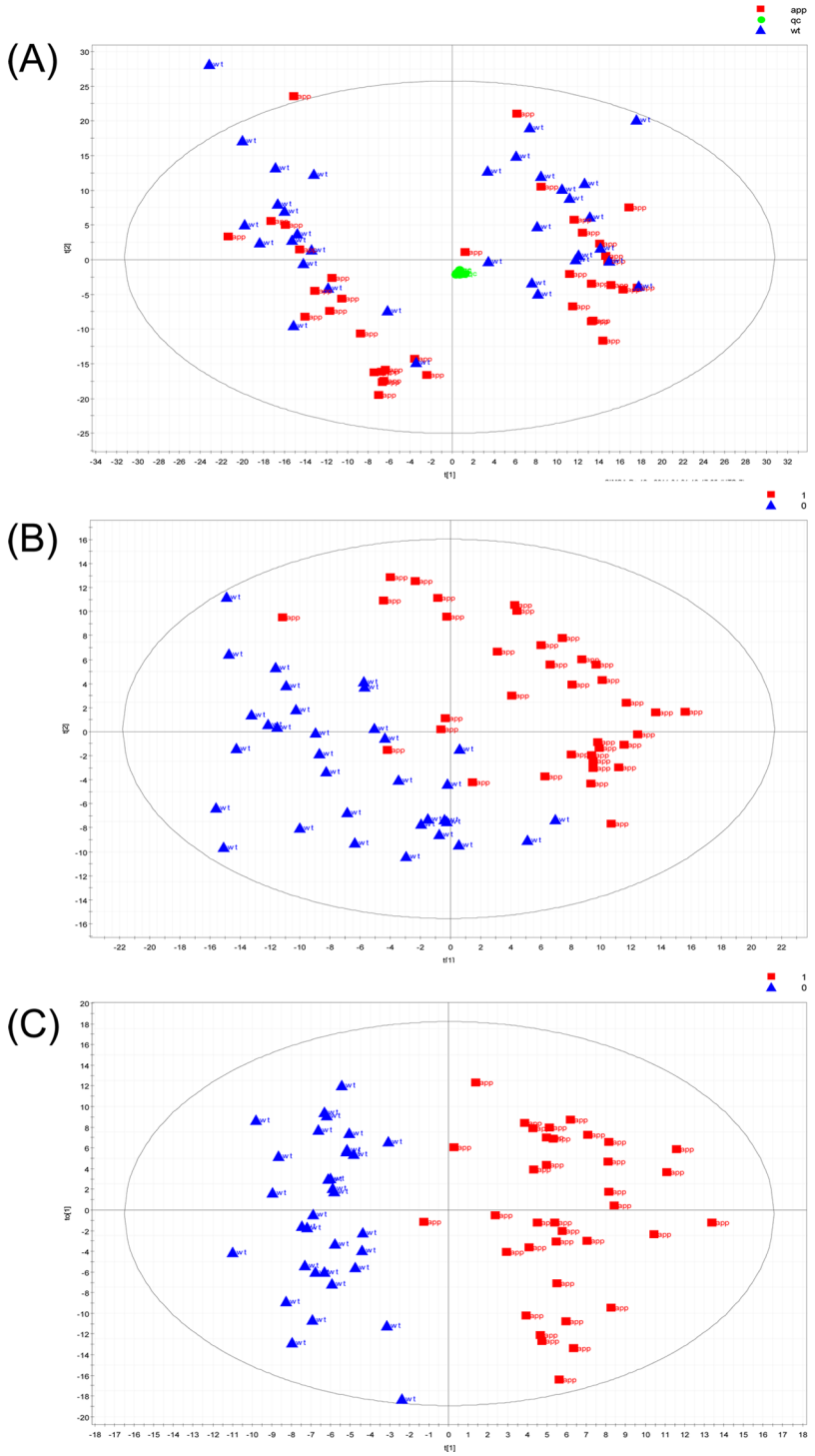

Figure 3. (A) PCA score plot of all the mice urine samples. Green dots were the eight injections of the quality control sample. Red boxes were labeled as mutant APP mice, and blue triangles were labeled as wild type mice. (B) PLS-DA score plot of all the mice urine samples. Red boxes were labeled as mutant APP mice, and blue triangles were labeled as wild type mice. $R^2Y(cum)$ was 0.719, and $Q^2(cum)$ was 0.516. (C) OPLS-DA score plot of all the mice urine samples. Red boxes were labeled as mutant APP mice, and blue triangles were labeled as wild type mice. $R^2Y(cum)$ was 0.854, and $Q^2(cum)$ was 0.665.

good reproducibility could be obtained by the isotope labeling LC−MS method.

Note that the differential isotope labeling LC−MS method is for relative quantification of metabolites in comparative samples. If needed, spiking a labeled metabolite standard with known concentration to a differentially labeled sample can be used for absolute quantification. However, for most metabolomics studies, determining the metabolic changes or relative quantification of metabolites is more important. Differential isotope labeling LC−MS uses peak ratio values of peak pairs to perform relative quantification which is more precise than using absolute signal intensity of peaks. For example, we randomly selected three metabolites (high, middle, and low abundant metabolites) in the eight quality control samples. Supporting

dx.doi.org/10.1021/pr500828v | J. Proteome Res. 2014, 13, 4457−4469

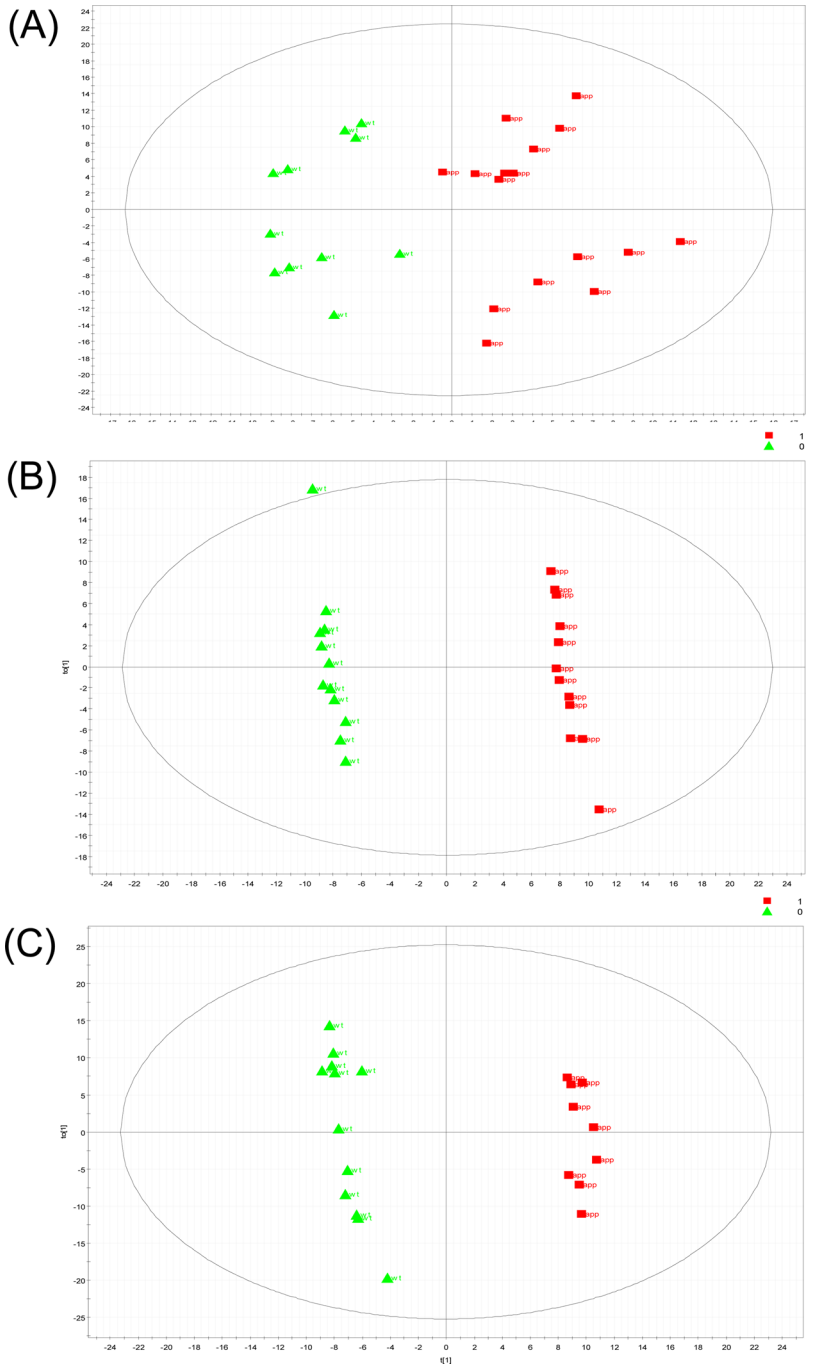

Figure 4. Score plots of OPLS-DA at (A) the age of 15−17 weeks, (B) the age of 25−28 weeks, and (C) the age of 30−31 weeks.

Information Table T4 shows that the RSD of the absolute intensity of these three metabolites was 14%, 30%, and 28%. In contrast, the RSD of the relative intensity ($^{12}C/^{13}C$ ratio) of the three metabolites was 2.4%, 1.9%, and 3.9%.

Comparative Metabolome Analysis in Mouse Model of AD

PCA, an unsupervised chemometric method, was used to obtain an overall picture of the whole data sets, and to see if there was any clustering, trends, or outliers. Figure 3A shows the PCA score plot of all the urine samples labeled as QC samples (in green), APP mutant group (in red), and wild type group (in blue). The eight QC injections cluster together closely, indicating that our method was sufficiently robust that the quality of the whole LC−MS data for this study should be satisfactory.[50] Figure 3A shows that there is a separation between APP mutant and wild type groups, although the separation is not distinct. If we label the samples as male and female (see Supporting Information Figure S3), there is a clear separation between male and female mouse urine samples, which is consistent with the previous report.[51]

In order to maximize the separation between the APP mutant and wild type groups, we need to input a priori information about the two classes and use the supervised models, such as PLS-DA and OPLS-DA.[52,53] Figure 3B shows the PLS-DA score plot of urine samples between APP mutant and wild type groups. There is a clear separation between APP mutant and wild type groups, although there are a few overlapping data points between the two groups. OPLS-DA

dx.doi.org/10.1021/pr500828v | J. Proteome Res. 2014, 13, 4457−4469

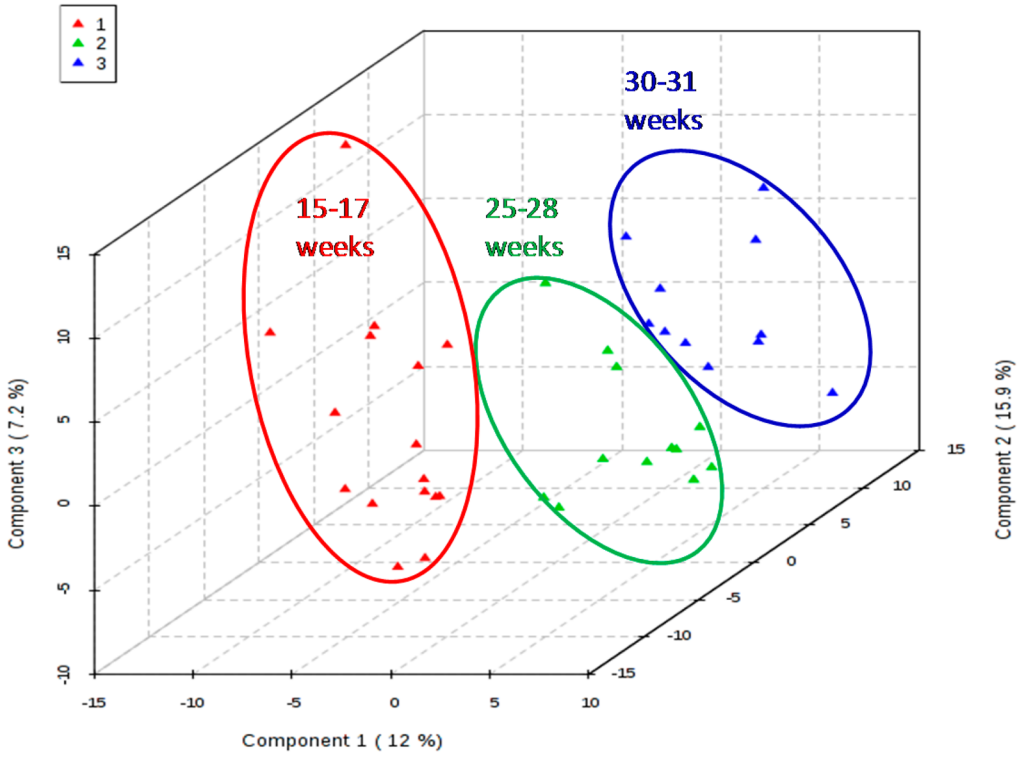

Figure 5. Prediction model showing the metabolic trajectory of three time points among the APP mice.

Table 2. List of Top 15 Important Metabolites Found in the Mouse Urine Samples That Differentiated the APP Mutant Group and the Wild Type Group

ret. time (min)	mass of dansylated metabolite	mass of metabolite	metabolite	mass accuracy (ppm)	ID[a]	fold change	*t* test (*p*-value)
21.48	400.12156	166.06323	desaminotyrosine	1.4	D	2.20	$10^{-5.6}$
12.47	337.15813	103.09980	choline	0.9	D	−2.00	0.00033
14.33	383.10911	149.05078	L-methionine	1.8	D	1.81	0.0028
18.71	425.11673	191.05840	5-hydroxyindoleacetic acid	0.8	D	−1.80	0.0010
2.91	359.07268	125.01435	taurine	2.5	D	−1.70	0.0090
20.98	327.64260	187.16853	N1-acetylspermidine	0.4	D	−1.50	0.0014
27.90	330.59553	193.07439	phenylacetylglycine or methylhippuric acid	2.5	P	2.20	0.00045
16.87	348.10153	114.04320	dihydrouracil	2.3	P	2.19	$10^{-6.0}$
12.22	366.11202	132.05369	ureidopropionic acid	1.4	P	1.94	$10^{-5.5}$
15.67	401.06614	167.00781	thiocysteine	1.9	P	1.82	0.0050
26.71	317.58747	167.05828	hydroxyphenylglycine or pyridoxal	0.2	P	−1.60	0.00027
6.66	479.23249	245.17416	lysine-valine	1.1	P	−1.55	0.00034
28.14	341.06009	214.00353	unknown			2.35	0.0014
26.47	309.09803	75.03970	unknown			2.07	0.00012
9.42	362.11708	128.05875	unknown			2.00	0.00015

[a]D = definitely identified; P = putatively identified.

removes the unrelated variation in the data sets, such as gender in this case. Figure 3C shows that the OPLS-DA model could discriminate the APP mutant group from the wild type group. R^2 is used to evaluate the goodness of fitting, while Q^2 is used to evaluate the goodness of prediction. The OPLS-DA had R^2Y and Q^2Y values larger than 0.5, suggesting that it was a robust and predictable model (R^2X_{cum} = 0.513, R^2Y_{cum} = 0.854, Q^2Y_{cum} = 0.665 for one predictive component and three orthogonal components). We did the cross validation for the PLS-DA and OPLS-DA models. Supporting Information Figure S4 shows the 20 permutation test for PLS-DA model. The slopes of both R and Q are positive and permutation data in the left are lower than the original point on the right top, which suggests that the model was valid. The CV-ANOVA, a built-in cross validation method in SIMCA-P, was used to do the cross validation of the OPLS-DA model, and it showed the model was robust (data not shown).

Since the mouse urine samples were collected at three different time points, we also divided the data into three individual time points and performed the OPLS-DA analysis. Figure 4 shows that the OPLS-DA can separate the APP mutant group and the wild type group in each of three time points. The separations between the APP mutant and the wild type group at 25−28 weeks and at 30−31 weeks are similar (Q^2

dx.doi.org/10.1021/pr500828v | J. Proteome Res. 2014, 13, 4457−4469

= 0.75), and they both are more pronounced than that at 15−17 weeks (Q^2 = 0.40). This observation can be explained by the phenotype change of amyloid plaques in the APP mutant mouse brain with time. The amyloid plaques appear as early as 2−3 months and become more dense at 6 months.[43,54]

We have also constructed a prediction model in a 3D plot to trace the progression of three time points (three groups) among the APP mice samples (see Figure 5). Figure 5 shows that there is a clear metabolomic trajectory changing from 15−17 weeks, to 25−28 weeks, and to 30−31 weeks. The changes from 15−17 weeks to 25−28 weeks are more pronounced than that from 25−28 weeks to 30−31 weeks.

Identification of Candidate Metabolite Biomarkers

Metabolite identification is a challenging and time-consuming process.[38] We focused on a relatively short list of candidate metabolites for identification. The top 15 most important metabolites were selected from the loading plot based on their variable importance in the project value and they were also validated by Student's *t* test. Table 2 shows a list of these top 15 metabolites with their retention time, accurate mass of dansylated metabolite, accurate mass of underivatized metabolite, mass accuracy error, fold change, and *p*-value. The use of high resolution and high mass accuracy FTICR−MS permitted the use of a small mass error tolerance window, 5 ppm, to perform mass search in a metabolome database and gave us a relatively short list of possible hits. Furthermore, the MS/MS spectrum was used to facilitate the identification of the potential metabolites. As an example, Figure 6 shows the MS/MS spectra of ^{12}C-danylated and ^{13}C-dansylated methionine in the mouse sample matched with those of the reference standard.

In this work, methionine, desaminotyrosine, taurine, N1-acetylspermidine, 5-hydroxyindoleacetic acid, and choline were definitely identified. Dihydrouracil, lysine-valine, thiocysteine, and ureidopropionic acid were putatively identified. The remaining significant metabolites could not be identified. Figure 7 shows the change of relative concentration level of some metabolites in the APP mutant group and the wild type group at three different ages of 15−17 weeks, 25−28 weeks, and 30−31 weeks. We can see that methionine and desaminotyrosine are upregulated and N1-acetylspermidine and 5-hydroxyindoleacetic acid are downregulated in the APP mutant group. They show some differences among the three different ages within the wild type group, but these metabolites show more significant differences from the APP mutant group. The differences between the APP mutant and the wild type group for all these metabolites at each three different ages are statistically significant, and the *p*-values are all <0.001.

Significance of Candidate Metabolite Biomarkers

The metabolomic profile changes as shown in Figures 4 and 5 and the relative concentration changes of individual metabolites as shown in Figure 7 are significant for understanding the AD disease development. The metabolomic changes between the APP mutant group and the wild type group may be used in the future to examine the efficacy of a treatment at any time point of the disease development; a reversal of metabolomic changes to the normal control would indicate that a treatment could reverse the disease development process. In addition, if some of the metabolite biomarkers are transferable to human samples, they could potentially be served as biomarkers for disease diagnosis or monitoring therapeutic efficacy in human. The

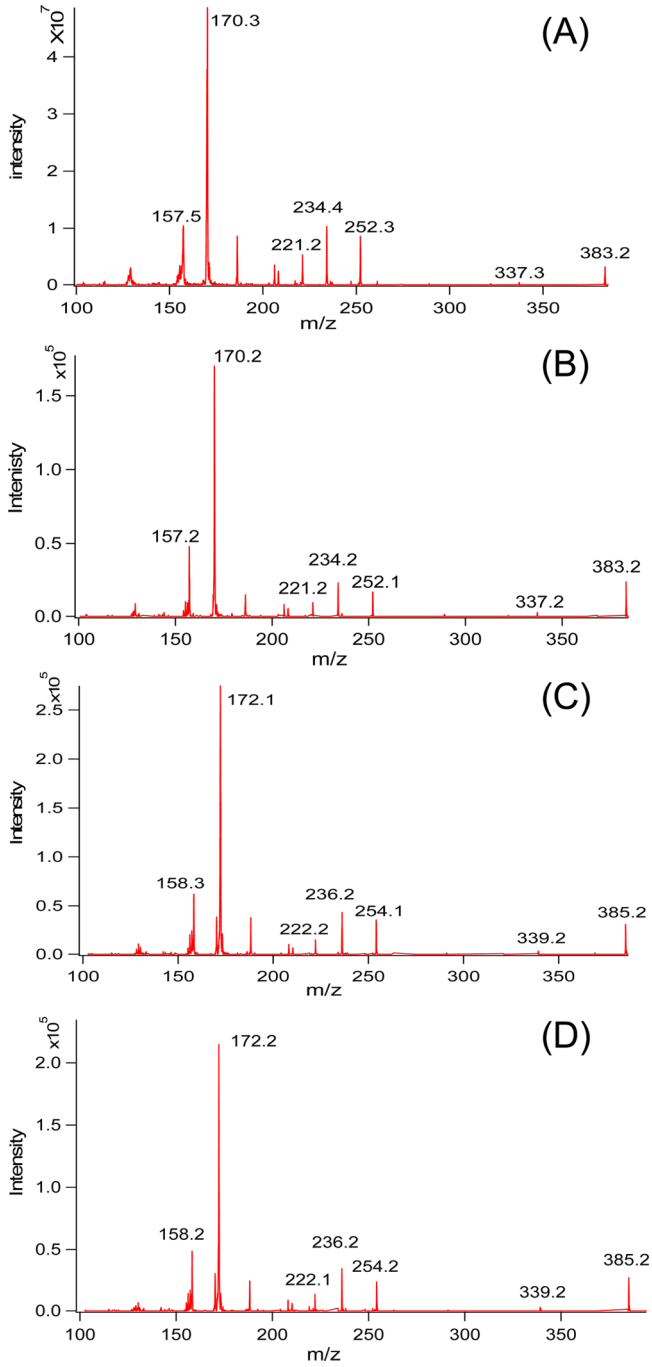

Figure 6. MS/MS spectra of (A) ^{12}C-dansylated methionine standard, (B) ^{12}C-dansylated methionine in the mouse urine sample, (C) ^{13}C-dansylated methionine standard, and (D) ^{13}C-dansylated methionine in the mouse urine sample.

biological significances of the potential metabolite biomarkers found in this mouse model study are briefly discussed below.

Methionine is an essential amino acid containing sulfur, which mouse could not synthesize. Homocysteine also containing sulfur is an intermediate product in the methionine metabolism pathway. The elevated level of blood plasma homocysteine was reported to be associated with high risk of AD.[55,56] A methionine-rich diet could cause high level of plasma homocysteine, which resulted in the acceleration of brain Aβ accumulation in the APP mutant mouse.[57] In methionine metabolism pathway, methionine can be converted

dx.doi.org/10.1021/pr500828v | J. Proteome Res. 2014, 13, 4457−4469

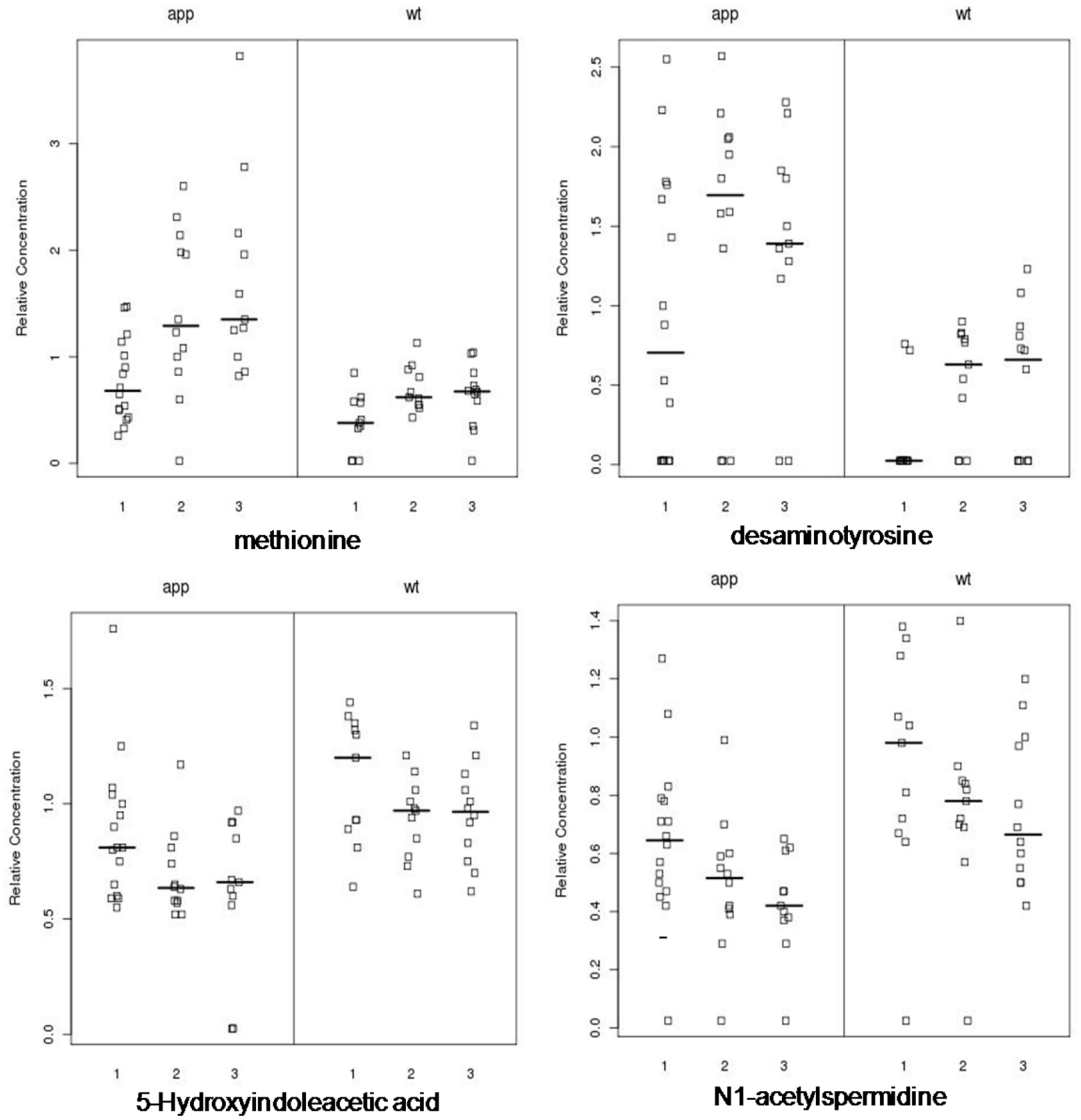

Figure 7. Plots showing the changed relative concentration level of candidate metabolite biomarkers in the APP mutant (app) and wild type (wt) groups at three different ages: 1 corresponds to 15−17 weeks, 2 corresponds to 25−28 weeks, and 3 corresponds to 30−31 weeks. The horizontal dark line is the median value. The *p*-value of the difference between the mutant APP and wild type groups at each of three ages was calculated to be <0.001 for these metabolites.

to *S*-adenosylmethionine (SAM), which serves as ubiquitous methyl group donor and is necessary for the synthesis of neurotransmitters, neuronal membrane stability, and DNA methylation. A decreased level of SAM in CSF was reported to be associated with the AD patients.[58] Methionine is also required for synthesis of cysteine, and the sulfur atom from methionine is transferred to cysteine. We also observed that a putatively identified metabolite thiocysteine were upregulated in the mutant APP mice. Thiocysteine was an intermediate product in the cysteine metabolism pathway. In this study, we observed that the methionine and cysteine metabolism was disturbed, which provided evidence that methionine and cysteine metabolism pathway warrant further investigation for AD transgenic mice model. Interestingly, one recent metabolomics study in human CSF also showed that the methionine level was significantly increased in AD patients.[17] These results suggest that the methionine related pathway may play an important role in the pathophysiology of AD.

Taurine is also a sulfur amino acid, which can be synthesized by human body from cysteine. Taurine has many diverse biological functions serving as a neurotransmitter in the brain, a stabilizer of cell membranes, and a facilitator in the transport of ions. Recently, it was reported a relative decrease in the concentration of taurine in the frontal cortex and midbrain of the TgCRND8 APP 695 transgenic mouse, compared to the control.[20] Another recent study also reported reduction of taurine concentration in the Tg2576 AD in a mouse model.[32] In a study of human saliva metabolomics, it was found that taurine level was reduced in patients with mild cognitive impartment (MCI), a disease related to AD.[29] Consistent with previous studies, in our study we observed a decreased level of taurine in the mutant APP mouse urine samples.

The relative concentration of desaminotyrosine was increased in mutant APP mice. It is one of the phenolic acid metabolites of tyrosine by tyrosine aminotransferase.[59] There is very little literature information on the biological function of this metabolite. However, the tyrosine metabolism pathway is

dx.doi.org/10.1021/pr500828v | *J. Proteome Res.* 2014, 13, 4457−4469

important and some well-known neurotransmitters, such as L-Dopa, dopamine, are derivatized from tyrosine. Further investigation of desamiontyrosine is needed to find out what role it plays in the metabolite pathway related to AD disease.

N1-Acetylspermidine is one of aliphatic polyamines occurring ubiquitously in organisms. Polyamines have important functions in the stabilization of cell membranes, biosynthesis of informing molecules, and cell growth and differentiation. Reduced concentration of N1-acetylspermidine was previously reported in the urine of AD patients by a traditional biochemical study method.[60] In our work, a reduced level of N1-acetylspermidine in the transgenic mouse model of AD was observed.

5-Hydroxyindoleacetic acid is a metabolite of serotonin which is one of the important neurotransmitters in the brain. Neurotransmitters react with receptors in the postsynaptic membrane, thereby activating the neuron and transmitting the signal. The concentration changes of several neurotransmitters including serotonin were implicated in AD.[61] Although there was no change observed in the human brain tissue, a decreased level of 5-hydroxyindoleacetic acid in human CSF samples was reported to be associated with AD by traditional biochemistry study.[62,63] One recent metabolomics study also showed that 5-hydroxyindoleacetic acid was dysregulated in human CSF samples of AD patients.[13] In this work, we observed that 5-hydroxyindoleacetic acid level was changed in the APP mutant urine samples, which provides further evidence that serotonin metabolic pathway is likely to be associated with the pathology of AD.

Choline is an important metabolite since it serves as a precursor of acetylcholine, as a methyl donor in various metabolic processes. We found that the level change of choline may be involved in AD. Our result was also in agreement with another recent metabolomics study in human CSF samples, in which they identified choline as a potential disease progress biomarker.[25]

The findings of these potentially biological relevant metabolites, as discussed above, demonstrated that our metabolomic profiling method could be useful in untargeted metabolomic biomarker discovery. In addition, some candidate metabolites, such as methionine, 5-hydroxyindoleacetic acid, choline, and taurine, identified in this mouse model study are in agreement with previous metabolomics studies in human CSF and blood samples. Although urine is not in close proximity to brain tissue, it might reflect the systems body response to AD. Urine metabolomics may have potential to be a noninvasive diagnostic tool for AD. Furthermore, urine metabolomics may also be used to assess the therapeutic intervention for the management and treatment of AD, particularly at the early stage of the disease development.

CONCLUSIONS

We have developed a new LC−MS method for analyzing the mouse urine metabolome with much improved metabolome coverage. This method allowed us to detect and quantify more than 950 metabolites in mouse urine samples using a starting material of 20 μL. From eight LC−MS runs of the quality control sample prepared from a pooled urine sample, a total of 1454 peak pairs could be detected and 92% of them could match with the metabolites in either the HMDB database or the EML library based on accurate mass search. Urinary metabolomic study on a transgenic mice model of AD showed that metabolomic profiles could differentiate the mutant APP from the wild type mice. Several metabolite candidate biomarkers identified in this work were consistent with previous metabolomics study in human CSF. Our study indicated that, complementary to CSF, brain, and plasma, urine has the potential to be used to search for noninvasive, inexpensive, sensitive metabolic biomarkers for AD disease diagnosis and also therapeutic effect monitoring.

One of the limitations in this study is that dansylation labeling mainly enhanced the detection of the compounds containing primary, secondary amines and phenol groups, but it could not detect some other class of compounds like glucose and fatty acids, which might be interesting to AD. This limitation will be overcome by using other isotopic labeling reagents. For example, isotope-coded *p*-dimethylaminophenacyl bromide can be used to detect compounds containing carboxylic groups.[47] We plan to apply these newly developed labeling methods to comprehensively study the mouse urine metabolome in order to obtain the whole picture of metabolic perturbations in the transgenic mouse of AD (i.e., detecting more metabolites in each metabolic network) for better understanding of the disease and searching for more specific and sensitive biomarkers for early diagnosis of AD.

ASSOCIATED CONTENT

Supporting Information

Extracted ion chromatograms for two labeled metabolites (Figure S1), base-peak ion chromatograms of three experimental replicates of labeled mouse urine (Figure S2), PCA score plot of male and female mice (Figure S3), PLS-DA model validation (Figure S4), summary of HMDB and EML database matches for QC samples (Table T1), list of matched metabolites to HMDB (Table T2), list of matched metabolites to EML (Table T3), and precision of retention time, mass measurement, and ion intensity of three metabolites from QC samples (Table T4). This material is available free of charge via the Internet at http://pubs.acs.org.

AUTHOR INFORMATION

Corresponding Author

*E-mail: Liang.Li@ualberta.ca. Tel: 780-492-3250. Fax: 780-492-8231.

Notes

The authors declare no competing financial interest.

ACKNOWLEDGMENTS

This work was funded by the Natural Sciences and Engineering Research Council of Canada, Canadian Institutes of Health Research, the Canada Research Chairs program, the Canada Foundation for Innovation, the Alberta Prion Research Institute, Genome Canada, and Genome Alberta.

REFERENCES

(1) Bishop, N. A.; Lu, T.; Yankner, B. A. Neural mechanisms of ageing and cognitive decline. *Nature* **2010**, *464* (7288), 529−535.
(2) Lovestone, S. Searching for biomarkers in neurodegeneration. *Nat. Med.* **2010**, *16* (12), 1371−1372.
(3) Gupta, V. B.; Sundaram, R.; Martins, R. N. Multiplex biomarkers in blood. *Alzheimer's Res. Ther.* **2013**, *5* (3), 6.
(4) Grossman, M. Multimodal Comparative Studies of Neurodegenerative Diseases. *J. Alzheimer's Dis.* **2013**, *33*, S379−S383.

(5) Kaddurah-Daouk, R.; Krishnan, K. R. R. Metabolomics: A Global Biochemical Approach to the Study of Central Nervous System Diseases. *Neuropsychopharmacology* **2009**, *34* (1), 173−186.
(6) Quinones, M. P.; Kaddurah-Daouk, R. Metabolomics tools for identifying biomarkers for neuropsychiatric diseases. *Neurobiol. Dis.* **2009**, *35* (2), 165−176.
(7) Mishur, R. J.; Rea, S. L. Applications of mass spectrometry to metabolomics and metabonomics: Detection of biomarkers of aging and of age-related diseases. *Mass Spectrom. Rev.* **2012**, *31* (1), 70−95.
(8) Bierer, L. M.; Haroutunian, V.; Gabriel, S.; Knott, P. J.; Carlin, L. S.; Purohit, D. P.; Perl, D. P.; Schmeidler, J.; Kanof, P.; Davis, K. L. Neurochemical Correlates of Dementia Serverity in Alzheimers Disease - Relative Importance of the Cholinergic Deficits. *J. Neurochem.* **1995**, *64* (2), 749−760.
(9) Kapogiannis, D.; Mattson, M. P. Disrupted energy metabolism and neuronal circuit dysfunction in cognitive impairment and Alzheimer's disease. *Lancet Neurol.* **2011**, *10* (2), 187−198.
(10) Butterfield, D. A. beta-Amyloid-associated free radical oxidative stress and neurotoxicity: Implications for Alzheimer's disease. *Chem. Res. Toxicol.* **1997**, *10* (5), 495−506.
(11) Manczak, M.; Anekonda, T. S.; Henson, E.; Park, B. S.; Quinn, J.; Reddy, P. H. Mitochondria are a direct site of A beta accumulation in Alzheimer's disease neurons: Implications for free radical generation and oxidative damage in disease progression. *Hum. Mol. Genet.* **2006**, *15* (9), 1437−1449.
(12) Kaddurah-Daouk, R.; Rozena, S.; Matson, W.; Han, X.; Hulette, C. M.; Burke, J. R.; Doraiswamy, P. M.; Welsh-Bohmer, K. A. Metabolomic changes in autopsy-confirmed Alzheimer's disease. *Alzheimer's Dementia* **2010**, 1−9.
(13) Kaddurah-Daouk, R.; Zhu, H.; Sharma, S.; Bogdanov, M.; Rozen, S. G.; Matson, W.; Oki, N. O.; Motsinger-Reif, A. A.; Churchill, E.; Lei, Z.; Appleby, D.; Kling, M. A.; Trojanowski, J. Q.; Doraiswamy, P. M.; Arnold, S. E. Pharmacometabolomics Res, N., Alterations in metabolic pathways and networks in Alzheimer's disease. *Transl. Psychiatry* **2013**, *3*, 8.
(14) Ibanez, C.; Simo, C.; Barupal, D. K.; Fiehn, O.; Kivipelto, M.; Cedazo-Minguez, A.; Cifuentes, A. A new metabolomic workflow for early detection of Alzheimer's disease. *J. Chromatogr. A* **2013**, *1302*, 65−71.
(15) Trushina, E.; Dutta, T.; Persson, X. M. T.; Mielke, M. M.; Petersen, R. C. Identification of Altered Metabolic Pathways in Plasma and CSF in Mild Cognitive Impairment and Alzheimer's Disease Using Metabolomics. *PLoS One* **2013**, *8* (6), 13.
(16) Greenberg, N.; Grassano, A.; Thambisetty, M.; Lovestone, S.; Legido-Quigley, C. A proposed metabolic strategy for monitoring disease progression in Alzheimer's disease. *Electrophoresis* **2009**, *30* (7), 1235−1239.
(17) Oresic, M.; Hyotylainen, T.; Herukka, S. K.; Sysi-Aho, M.; Mattila, I.; Seppanan-Laakso, T.; Julkunen, V.; Gopalacharyulu, P. V.; Hallikainen, M.; Koikkalainen, J.; Kivipelto, M.; Helisalmi, S.; Lotjonen, J.; Soininen, H. Metabolome in progression to Alzheimer's disease. *Transl. Psychiatry* **2011**, *1*, 9.
(18) Li, N. J.; Liu, W. T.; Li, W.; Li, S. Q.; Chen, X. H.; Bi, K. S.; He, P. Plasma metabolic profiling of Alzheimer's disease by liquid chromatography/mass spectrometry. *Clin. Biochem.* **2010**, *43* (12), 992−997.
(19) Graham, S. F.; Chevallier, O. P.; Roberts, D.; Holscher, C.; Elliott, C. T.; Green, B. D. Investigation of the Human Brain Metabolome to Identify Potential Markers for Early Diagnosis and Therapeutic Targets of Alzheimer's Disease. *Anal. Chem.* **2013**, *85* (3), 1803−1811.
(20) Salek, R. M.; Xia, J.; Innes, A.; Sweatman, B. C.; Adalbert, R.; Randle, S.; McGowan, E.; Emson, P. C.; Griffin, J. L. A metabolomic study of the CRND8 transgenic mouse model of Alzheimer's disease. *Neurochem. Int.* **2010**, *56* (8), 937−947.
(21) Lin, S. H.; Liu, H. D.; Kanawati, B.; Liu, L. F.; Dong, J. Y.; Li, M.; Huang, J. D.; Schmitt-Kopplin, P.; Cai, Z. W. Hippocampal metabolomics using ultrahigh-resolution mass spectrometry reveals neuroinflammation from Alzheimer's disease in CRND8 mice. *Anal. Bioanal. Chem.* **2013**, *405* (15), 5105−5117.
(22) Hurko, O.; Boudonck, K.; Gonzales, C.; Hughes, Z. A.; Jacobsen, J. S.; Reinhart, P. H.; Crowther, D. Ablation of the locus coeruleus increases oxidative stress in Tg-2576 transgenic but not wild-type mice. *Int. J. Alzheimer's Dis.* **2010**, *2010*, 864625.
(23) Hu, L. P.; Browne, E. R.; Liu, T.; Angel, T. E.; Ho, P. C.; Chan, E. C. Y. Metabonomic Profiling of TASTPM Transgenic Alzheimer's Disease Mouse Model. *J. Proteome Res.* **2012**, *11* (12), 5903−5913.
(24) Graham, S. F.; Holscher, C.; McClean, P.; Elliott, C. T.; Green, B. D. H-1 NMR metabolomics investigation of an Alzheimer's disease (AD) mouse model pinpoints important biochemical disturbances in brain and plasma. *Metabolomics* **2013**, *9* (5), 974−983.
(25) Ibanez, C.; Simo, C.; Martin-Alvarez, P. J.; Kivipelto, M.; Winblad, B.; Cedazo-Minguez, A.; Cifuentes, A. Toward a Predictive Model of Alzheimer's Disease Progression Using Capillary Electrophoresis-Mass Spectrometry Metabolomics. *Anal. Chem.* **2012**, *84* (20), 8532−8540.
(26) Guo, K.; Li, L. Differential C-12/C-13-Isotope Dansylation Labeling and Fast Liquid Chromatography/Mass Spectrometry for Absolute and Relative Quantification of the Metabolome. *Anal. Chem.* **2009**, *81* (10), 3919−3932.
(27) Guo, K.; Bamforth, F.; Li, L. Qualitative Metabolome Analysis of Human Cerebrospinal Fluid by C-13/C-12-Isotope Dansylation Labeling Combined with Liquid Chromatography Fourier Transform Ion Cyclotron Resonance Mass Spectrometry. *J. Am. Soc. Mass Spectrom.* **2011**, *22* (2), 339−347.
(28) Wu, Y.; Li, L. Determination of Total Concentration of Chemically Labeled Metabolites as a Means of Metabolome Sample Normalization and Sample Loading Optimization in Mass Spectrometry-Based Metabolomics. *Anal. Chem.* **2012**, *84* (24), 10723−10731.
(29) Zheng, J. M.; Dixon, R. A.; Li, L. Development of Isotope Labeling LC−MS for Human Salivary Metabolomics and Application to Profiling Metabolome Changes Associated with Mild Cognitive Impairment. *Anal. Chem.* **2012**, *84* (24), 10802−10811.
(30) Wu, Y.; Li, L. Development of isotope labeling liquid chromatography-mass spectrometry for metabolic profiling of bacterial cells and its application for bacterial differentiation. *Anal. Chem.* **2013**, *85* (12), 5755−5763.
(31) Fu, F.; Cheng, V. W. T.; Wu, Y.; Tang, Y.; Weiner, J. H.; Li, L. Comparative Proteomic and Metabolomic Analysis of Staphylococcus warneri SG1 Cultured in the Presence and Absence of Butanol. *J. Proteome Res.* **2013**, *12* (10), 4478−4489.
(32) Fukuhara, K.; Ohno, A.; Ota, Y.; Senoo, Y.; Maekawa, K.; Okuda, H.; Kurihara, M.; Okuno, A.; Niida, S.; Saito, Y.; Takikawa, O. NMR-based metabolomics of urine in a mouse model of Alzheimer's disease: identification of oxidative stress biomarkers. *J. Clin. Biochem. Nutr.* **2013**, *52* (2), 133−138.
(33) Bando, K.; Kawahara, R.; Kunimatsu, T.; Sakai, J.; Kimura, J.; Funabashi, H.; Seki, T.; Bamba, T.; Fukusaki, E. Influences of biofluid sample collection and handling procedures on GC-MS based metabolomic studies. *J. Biosci. Bioeng.* **2010**, *110* (4), 491−499.
(34) Smith, C. A.; Want, E. J.; O'Maille, G.; Abagyan, R.; Siuzdak, G. XCMS: Processing mass spectrometry data for metabolite profiling using Nonlinear peak alignment, matching, and identification. *Anal. Chem.* **2006**, *78* (3), 779−787.
(35) Xia, J. G.; Psychogios, N.; Young, N.; Wishart, D. S. MetaboAnalyst: A web server for metabolomic data analysis and interpretation. *Nucleic Acids Res.* **2009**, *37*, W652−W660.
(36) Wishart, D. S.; Knox, C.; Guo, A. C.; Eisner, R.; Young, N.; Gautam, B.; Hau, D. D.; Psychogios, N.; Dong, E.; Bouatra, S.; Mandal, R.; Sinelnikov, I.; Xia, J. G.; Jia, L.; Cruz, J. A.; Lim, E.; Sobsey, C. A.; Shrivastava, S.; Huang, P.; Liu, P.; Fang, L.; Peng, J.; Fradette, R.; Cheng, D.; Tzur, D.; Clements, M.; Lewis, A.; De Souza, A.; Zuniga, A.; Dawe, M.; Xiong, Y. P.; Clive, D.; Greiner, R.; Nazyrova, A.; Shaykhutdinov, R.; Li, L.; Vogel, H. J.; Forsythe, I. HMDB: A knowledgebase for the human metabolome. *Nucleic Acids Res.* **2009**, *37*, D603−D610.

(37) Li, L.; Li, R. H.; Zhou, J. J.; Zuniga, A.; Stanislaus, A. E.; Wu, Y. M.; Huan, T.; Zheng, J. M.; Shi, Y.; Wishart, D. S.; Lin, G. H. MyCompoundID: Using an Evidence-Based Metabolome Library for Metabolite Identification. *Anal. Chem.* **2013**, *85* (6), 3401−3408.
(38) Baker, M. Metabolomics: from small molecules to big ideas. *Nat. Methods* **2011**, *8* (2), 117−121.
(39) Barba, I.; Fernandez-Montesinos, R.; Garcia-Dorado, D.; Pozo, D. Alzheimer's disease beyond the genomic era: nuclear magnetic resonance (NMR) spectroscopy-based metabolomics. *J. Cell. Mol. Med.* **2008**, *12* (5A), 1477−1485.
(40) Janus, C.; Chishti, M. A.; Westaway, D. Transgenic mouse models of Alzheimer's disease. *Biochim. Biophys. Acta, Mol. Basis Dis.* **2000**, *1502* (1), 63−75.
(41) Kokjohn, T. A.; Roher, A. E. Amyloid precursor protein transgenic mouse models and Alzheimer's disease: Understanding the paradigms, limitations, and contributions. *Alzheimer's Dementia* **2009**, *5* (4), 340−347.
(42) Phinney, A. L.; Horne, P.; Yang, J.; Janus, C.; Bergeron, C.; Westaway, D. Mouse models of Alzheimer's disease: The long and filamentous road. *Neurol. Res.* **2003**, *25* (6), 590−600.
(43) Chishti, M. A.; Yang, D. S.; Janus, C.; Phinney, A. L.; Horne, P.; Pearson, J.; Strome, R.; Zuker, N.; Loukides, J.; French, J.; Turner, S.; Lozza, G.; Grilli, M.; Kunicki, S.; Morissette, C.; Paquette, J.; Gervais, F.; Bergeron, C.; Fraser, P. E.; Carlson, G. A.; St George-Hyslop, P.; Westaway, D. Early-onset amyloid deposition and cognitive deficits in transgenic mice expressing a double mutant form of amyloid precursor protein 695. *J. Biol. Chem.* **2001**, *276* (24), 21562−21570.
(44) Bateman, R. J.; Xiong, C. J.; Benzinger, T. L. S.; Fagan, A. M.; Goate, A.; Fox, N. C.; Marcus, D. S.; Cairns, N. J.; Xie, X. Y.; Blazey, T. M.; Holtzman, D. M.; Santacruz, A.; Buckles, V.; Oliver, A.; Moulder, K.; Aisen, P. S.; Ghetti, B.; Klunk, W. E.; McDade, E.; Martins, R. N.; Masters, C. L.; Mayeux, R.; Ringman, J. M.; Rossor, M. N.; Schofield, P. R.; Sperling, R. A.; Salloway, S.; Morris, J. C. Clinical and Biomarker Changes in Dominantly Inherited Alzheimer's Disease. *N. Engl. J. Med.* **2012**, *367* (9), 795−804.
(45) Mak, T. D.; Laiakis, E. C.; Goudarzi, M.; Fornace, A. J. MetaboLyzer: A Novel Statistical Workflow for Analyzing Post-processed LC−MS Metabolomics Data. *Anal. Chem.* **2014**, *86* (1), 506−513.
(46) Goudarzi, M.; Weber, W.; Mak, T. D.; Chung, J.; Doyle-Eisele, M.; Melo, D.; Brenner, D. J.; Guilmette, R. A.; Fornace, A. J., Jr. Development of Urinary Biomarkers for Internal Exposure by Cesium-137 Using a Metabolomics Approach in Mice. *Radiat. Res.* **2014**, *181* (1), 54−64.
(47) Guo, K.; Li, L. High-Performance Isotope Labeling for Profiling Carboxylic Acid-Containing Metabolites in Biofluids by Mass Spectrometry. *Anal. Chem.* **2011**, *82* (21), 8789−8793.
(48) Crews, B.; Wikoff, W. R.; Patti, G. J.; Woo, H. K.; Kalisiak, E.; Heideker, J.; Siuzdak, G. Variability Analysis of Human Plasma and Cerebral Spinal Fluid Reveals Statistical Significance of Changes in Mass Spectrometry-Based Metabolomics Data. *Anal. Chem.* **2009**, *81* (20), 8538−8544.
(49) Gika, H. G.; Macpherson, E.; Theodoridis, G. A.; Wilson, I. D. Evaluation of the repeatability of ultra-performance liquid chromatography-TOF-MS for global metabolic profiling of human urine samples. *J. Chromatogr. B: Anal. Technol. Biomed. Life Sci.* **2008**, *871* (2), 299−305.
(50) Want, E. J.; Wilson, I. D.; Gika, H.; Theodoridis, G.; Plumb, R. S.; Shockcor, J.; Holmes, E.; Nicholson, J. K. Global metabolic profiling procedures for urine using UPLC−MS. *Nat. Protoc.* **2010**, *5* (6), 1005−1018.
(51) Plumb, R.; Granger, J.; Stumpf, C.; Wilson, I. D.; Evans, J. A.; Lenz, E. M. Metabonomic analysis of mouse urine by liquid-chromatography-time of flight mass spectrometry (LC-TOFMS): detection of strain, diurnal and gender differences. *Analyst* **2003**, *128* (7), 819−823.
(52) Trygg, J.; Holmes, E.; Lundstedt, T. Chemometrics in metabonomics. *J. Proteome Res.* **2007**, *6* (2), 469−479.
(53) Madsen, R.; Lundstedt, T.; Trygg, J. Chemometrics in metabolomics—A review in human disease diagnosis. *Anal. Chim. Acta* **2010**, *659* (1−2), 23−33.
(54) Vardarajan, B.; Vergote, D.; Tissir, F.; Logue, M.; Yang, J.; Daude, N.; Ando, K.; Rogaeva, E.; Lee, J.; Cheng, R.; Brion, J. P.; Ghani, M.; Shi, B. P.; Baldwin, C. T.; Kar, S.; Mayeux, R.; Fraser, P.; Goffinet, A. M.; George-Hyslop, P., St; Farrer, L. A.; Westaway, D. Role of p73 in Alzheimer disease: Lack of association in mouse models or in human cohorts. *Mol. Neurodegener.* **2013**, *8*, 10.
(55) Popp, J.; Lewczuk, P.; Linnebank, M.; Cvetanovska, G.; Smulders, Y.; Kolsch, H.; Frommann, I.; Kornhuber, J.; Maier, W.; Jessen, F. Homocysteine Metabolism and Cerebrospinal Fluid Markers for Alzheimer's Disease. *J. Alzheimer's Dis.* **2009**, *18* (4), 819−828.
(56) McCampbell, A.; Wessner, K.; Marlatt, M. W.; Wolffe, C.; Toolan, D.; Podtelezhnikov, A.; Yeh, S.; Zhang, R.; Szczerba, P.; Tanis, K. Q.; Majercak, J.; Ray, W. J.; Savage, M. Induction of Alzheimer's-like changes in brain of mice expressing mutant APP fed excess methionine. *J. Neurochem.* **2011**, *116* (1), 82−92.
(57) Zhuo, J. M.; Pratico, D. Normalization of hyperhomocysteinemia improves cognitive deficits and ameliorates brain amyloidosis of a transgenic mouse model of Alzheimer's disease. *FASEB J.* **2010**, *24* (10), 3895−3902.
(58) Linnebank, M.; Popp, J.; Smulders, Y.; Smith, D.; Semmler, A.; Farkas, M.; Kulic, L.; Cvetanovska, G.; Blom, H.; Stoffel-Wagner, B.; Kolsch, H.; Weller, M.; Jessen, F. S-Adenosylmethionine Is Decreased in the Cerebrospinal Fluid of Patients with Alzheimer's Disease. *Neurodegener. Dis.* **2009**, *7* (6), 373−378.
(59) Booth, A. N.; Masri, M. S.; Robbins, D. J.; Emerson, O. H.; Jones, F. T.; Deeds, F. Urinary Phenolic Acid Metabolites of Tyrosine. *J. Biol. Chem.* **1960**, *235* (9), 2649−2652.
(60) Paik, M. J.; Lee, S.; Cho, K. H.; Kim, K. R. Urinary polyamines and N-acetylated polyamines in four patients with Alzheimer's disease as their N-ethoxycarbonyl-N-pentafluoropropionyl derivatives by gas chromatography-mass spectrometry in selected ion monitoring mode. *Anal. Chim. Acta* **2006**, *576* (1), 55−60.
(61) Keverne, J.; Ray, M. Neurochemistry of Alzheimer's disease. *Psychiatry* **2005**, *4* (1), 40−42.
(62) Lopez, O. L.; Kaufer, D.; Reiter, C. T.; Carra, J.; DeKosky, S. T.; Palmer, A. M. Relationship between CSF neurotransmitter metabolites and aggressive behavior in Alzheimer's disease. *Eur. J. Neurol.* **1996**, *3* (2), 153−155.
(63) Sjogren, M.; Minthon, L.; Passant, U.; Blennow, K.; Wallin, A. Decreased monoamine metabolites in frontotemporal dementia and Alzheimer's disease. *Neurobiol. Aging* **1998**, *19* (5), 379−384.